

Article

Not peer-reviewed version

Gadolinium Complex with a Tris-Hydroxypyridinone as an Input for New Imaging Probes: Thermodynamic Stability, Molecular Modeling and Biodistribution

Inês Dias , [Lurdes Gano](#) , [Sílvia Chaves](#) ^{*} , [Maria Amélia Santos](#) ^{*}

Posted Date: 20 February 2025

doi: 10.20944/preprints202502.1574.v1

Keywords: hydroxypyridinones; MRI contrast agents; gadolinium-complex; thermodynamic stability; biodistribution



Preprints.org is a free multidisciplinary platform providing preprint service that is dedicated to making early versions of research outputs permanently available and citable. Preprints posted at Preprints.org appear in Web of Science, Crossref, Google Scholar, Scilit, Europe PMC.

Copyright: This open access article is published under a Creative Commons CC BY 4.0 license, which permit the free download, distribution, and reuse, provided that the author and preprint are cited in any reuse.

Article

Gadolinium Complex with a Tris-Hydroxypyridinone as an Input for New Imaging Probes: Thermodynamic Stability, Molecular Modeling and Biodistribution

Inês Dias ¹, Lurdes Gano ², Sílvia Chaves ^{1,*} and M. Amélia Santos ^{1,*}

¹ Centro de Química Estrutural, Institute of Molecular Sciences, Departamento de Engenharia Química, Instituto Superior Técnico, Universidade de Lisboa, Av. Rovisco Pais 1, 1049-001, Lisboa, Portugal

² Centro de Ciências e Tecnologias Nucleares, Instituto Superior Técnico, Universidade de Lisboa, CTN, Estrada Nacional 10 (km 139,7), LRS, Bobadela 2695-066, Portugal

* Correspondence: silvia.chaves@tecnico.ulisboa.pt (S.C.); masantos@tecnico.ulisboa.pt (M.A.S.)

Abstract: The development of gadolinium-based magnetic resonance imaging (MRI) contrast agents (CAs) is a highly challenging and demanding research field in metal-coordination medicinal chemistry. The recognized high capacity of hydroxypyridinone (HOPO)-based compounds to coordinate Gd(III) led us to evaluate a set of physico-chemical-biological properties of a new Gd(III)-complex with an hexadentate tripodal ligand (H₃L), containing three 3,4-HOPO chelating moieties attached to an anchoring cyclohexane backbone. In particular, the thermodynamic stability constants of the complex were evaluated by potentiometry, showing the formation of a high stable (1:1) Gd-L complex ($\log \beta_{\text{GdL}} = 26.59$), with full coordination even in acid-neutral pH conditions. Molecular simulations of the Gd(III) complex revealed a minimum energy structure with somehow distorted octahedral geometry, involving full metal hexa-coordination by the three bidentate moieties of the ligand arms, indicating that extra water molecules should be coordinated to the metal ion, an important feature for the CAs (required enhancement of water proton relaxivity). *In vivo* biodistribution studies with the ⁶⁷Ga complex, as surrogate of the corresponding Gd complex, showed *in vivo* stability and rapid excretion from the animal body. Though deserving further investigation, these results may give an input on future perspectives towards new MRI diagnostic agents.

Keywords: hydroxypyridinones; MRI contrast agents; gadolinium-complex; thermodynamic stability; biodistribution

1. Introduction

Paramagnetic metal ion complexes, mostly based on gadolinium (Gd(III)), have been investigated and used over the last three decades as magnetic resonance imaging (MRI) contrast agents (CAs) [1,2]. Gadolinium-based contrast agents (GBCAs) are now employed routinely to enhance the sensitivity and specificity of MRI examinations. The commercially available GBCAs are Gd(III) complexes with polyaminopolycarboxylate ligands enabling octadentate coordination to the metal ion and can be classified into two groups, according to the ligand structure: as macrocyclic (e.g. Dotarem) or as linear (e.g. Omniscan).

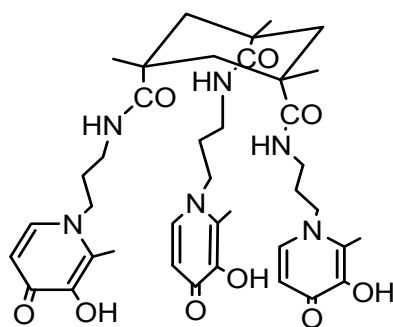
One of the major factors that controls the efficiency of MRI CAs is their relaxivity, that must be improved in order to reduce the amount of CA required. The relaxivity is the ability of the contrast to increase the relaxation rate of surrounding water protons, being mainly determined by the exchange rates between water molecules in the inner sphere and in the outer sphere. This includes the water of tissues and organs, though other parameters can affect the relaxivity of GBCAs such as the structure and molecular weight of the ligand, as well as their rotational correlation time [3].

Despite all the advantages of GBCAs, it is also crucial to take into consideration that gadolinium is very toxic as free ion, due to its recent association with nephrogenic systemic fibrosis [4]. Thus, for

clinical applications, a key aspect of the Gd(III) complexes used as CAs must be their high thermodynamic stability [5] as well as kinetic inertness. These properties are intended to guarantee the long-term resistance of the GBCAs to Gd(III) dissociation (and release of the toxic metal ion), for which the respective dissociation rate should be slower than the elimination rate in the patient body [6].

On the other hand, since the trivalent gadolinium prefers a coordination number of 9, its octadentate coordination with the currently available GBCAs, based on chelates with polyaminoacid ligands, leaves only one coordination site free for an inner sphere water molecule. Therefore, to improve the relaxivity by raising the hydration state of the contrast, the strategy of reducing the number of coordination sites provided by the ligands can be adopted, though for this family of Gd chelates it would imply both a reduction on the thermodynamic stability of the GBCAs as well as raised toxicity concerns. Aimed to overcome this problem, a new group of alternative Gd chelates were developed in 2006 by the group of K.N. Raymond [7], and in this line, a series of tripodal ligands containing three hydroxypyridinone (HOPO) chelating moieties, such as TREN-1-Me-3,2-HOPO, has been extensively investigated. The Gd(III) complexes with these ligands revealed to contain two or three water molecules coordinated to the metal ion, which conferred remarkable high relaxation efficiencies, besides high thermodynamic stability ($\log K_{GdL} = 19.2$) [7,8].

Following an identical strategy, different tripodal tris-3-hydroxy-4-pyridinone (tris-3,4-HOPOs) ligands were recently developed and evaluated for the magnetic and complexation properties of the corresponding Gd complexes [9,10]. The obtained results confirmed the capacity of these ligands to form very stable Gd complexes ($\log K_{GdHL} = 26.35$ [9], $\log K_{GdL} = 21.22$ [10]) with hexadentate coordination and two free sites left for water coordination to metal ion to enable efficient paramagnetic enhancement of water proton relaxation. Inspired by these findings, we have decided to investigate the properties of a Gd(III) complex with another tripodal tris-3,4-HOPO compound, KEMPPr(3,4-HP)₃ (see Scheme), having three 3,4-HOPO chelating moieties attached to cis,cis-1,3,5-trimethylcyclohexane-1,3,5-tricarboxylic acid (Kemp's triacid), which had previously revealed a high capacity to wrap and sequester three positive *hard* metal ions (Fe(III), Ga(III), Al(III)), through hexacoordination for the 1:1 M/L complexes [11]. In particular, herein are described the results of the studies on the chelating ability of KEMPPr(3,4-HP)₃ towards Gd(III), namely its solution equilibrium thermodynamic stability as a measure of its capacity to form strong hexa-coordinated 1:1 Gd/L complexes, and potentially leave extra positions for coordination of water molecules to Gd(III). Furthermore, molecular modeling calculations, based on density functional theory (DFT), were also performed to predict the probable metal complex structure and also the number of water molecules coordinated to Gd-complex; *in silico* evaluation was done as well to get some insight on some pharmacokinetic parameters of KEMPPr(3,4-HP)₃ and its metal complex. Finally, studies in mice were presented to assess the *in vivo* stability and biodistribution profile of the ⁶⁷Ga complex as a surrogate model of the analogue Gd-complex.



Scheme. Structural formula of the hexadentate tripodal compound KEMPPr(3,4-HP)₃.

2. Results and Discussion

2.1. Gd Chelation Studies

The determination of the thermodynamic stability constants of the Gd(III)-complex required a previous evaluation of the ligand protonation constants to be subsequently introduced in the Gd(III) complexation model. The acid-base behavior of KEMPPr(3,4-HP)₃ was already studied in aqueous medium [11], revealing that although the compound was isolated in the neutral tri-protonated form, H₃L, its fully protonated species (H₆L³⁺) has six dissociable protons. The three first protonation constants correspond to the phenolic groups of the 3,4-HP moieties while the last three are ascribed to the pyridyl nitrogen atoms. Although this compound is water soluble, the metal complexation studies revealed some solubility problems, namely due to the formation of the neutral M(III)L complexes as well as the possibility of precipitation due to metal hydrolysis. In fact, in the previously reported iron complexation studies with KEMPPr(3,4-HP)₃, a mixed medium (methanol/water) was also used to try to avoid these problems [11]. Therefore, herein it was decided to use a mixed DMSO/water medium (50%, w/w) and so the protonation constants had to be re-calculated under these experimental conditions, in order to introduce the corresponding acid-base data in the Gd(III) complexation model. Even though under the potentiometric experimental conditions some solubility problems can arise in aqueous medium, in cell studies the concentration of ligand used is lower (<7 μM) and thus the final DMSO concentration in culture media would be even lower (<1%), consequently not predicted to provoke substantial changes in biological tissues.

All the studies were performed by potentiometric titrations of the ligand alone or in the presence of a 1:1 Gd/L stoichiometric ratio (Figure 1), which allowed the determination of the protonation constants of KEMPPr(3,4-HP)₃, as well as the stability constants of the formed Gd(III)-complexes, from the best fitting of the experimental curves with the Hyperquad program [12] (Table 1). Other Gd to ligand molar ratios were not considered in the present study, because it was admitted that species with 1:2 stoichiometric ratio are present only at quite low concentrations for pH ca 7. In fact, in the previous evaluation of the Gd complexation model of another tripodal compound (NTP(PrHP)₃) [9], containing identical metal chelating hydroxypyridinone moieties, it was found that 1:2 species, namely GdH₃L₂, formed at pH 7 in percent concentration ca 2% under the experimental conditions used in the potentiometric titrations or 5% for C_L = 1 × 10⁻⁵ M (C_L/C_{Gd} = 10).

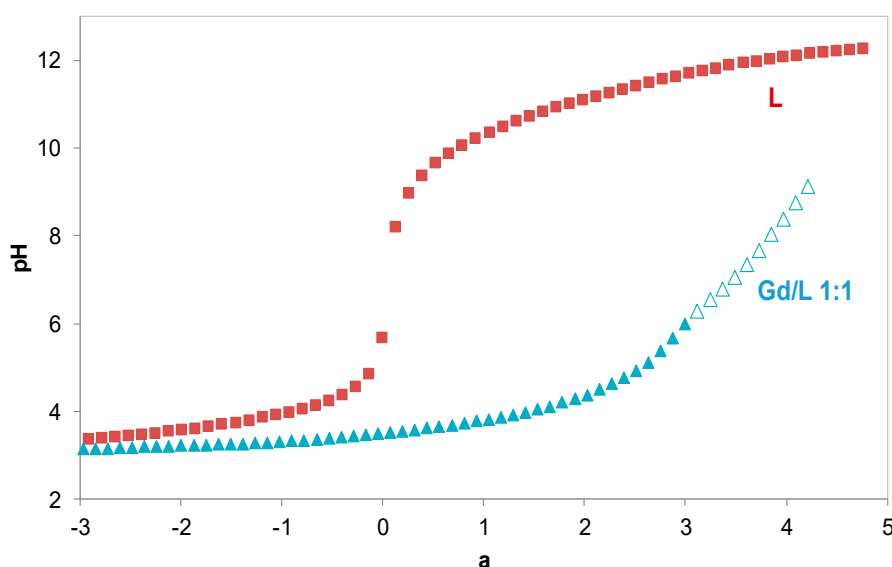
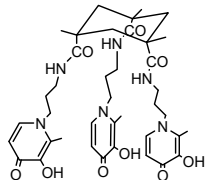
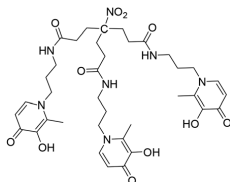
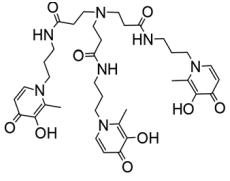


Figure 1. Potentiometric titration curves for the compound (H₃L), KEMPPr(3,4-HP)₃, and the system Gd(III)/L 1:1 (C_L = 3.2 × 10⁻⁴ M, 50% w/w DMSO/water medium); *a* represents moles of added base per mole of ligand. Empty symbols stand for experimental points that were not included in the calculations.

The herein obtained values for the protonation constants of $\text{KEMPPr}(3,4\text{-HP})_3$ are similar to those previously reported in aqueous medium for this and other tripodal compounds [10,11,13], though somehow higher values were found for the first three values probably due to the difference in the working media (50% w/w DMSO/water *vs* water). In fact, previous studies on the influence of the composition of DMSO/water media over acid-base equilibrium refer to the importance of the electrostatic forces [14,15]. Therefore, the basicity of negatively charged O-sites (from the HP moieties) is expected to increase with the lower hydrating capacity of the 50% w/w DMSO/water medium. Since the protonation centers contained in one arm of the tripodal ligand are quite far away from the similar ones in the remaining two arms, they can be considered equivalent basic groups, for which a difference in $\log K$ values of 0.602 could be expected [16]. In fact, a somehow higher difference (1.1) was found herein between $\log K_2$ and $\log K_3$, otherwise similar to a previously reported value (1.15) [10]) between $\log K_4$ and $\log K_5$ for H_3L_2 (Table 1), which can eventually result from the establishment of some hydrogen bond interactions and concomitant minor inequivalence between the arm protonation centers.

The species distribution plot in Figure 2 shows the predominance of the neutral H_3L species in the pH range 3.4-9.9, which means that at physiological pH (7.4) the composition of the solution is 99.95% of H_3L and only 0.05% of the monocharged H_4L^+ species.

Table 1. Stepwise protonation constants ($\log K_i$)^a, global formation constants^b of the Gd(III) complexes and pGd^c (50% w/w DMSO/water, $T = 25.0 \pm 0.1$ °C, $I = 0.1$ M KCl), as well as comparison values for some tripodal compounds.

Compound	$\log K_i$	(m,h,l)	$\log \beta(\text{Gd}_m\text{H}_h\text{L}_l)$
 KEMPPr(3,4-HP)₃	11.5(4)	(1,4,1)	41.35(8)
	10.97(5)	(1,2,1)	35.17(7)
	9.87(6)	(1,1,1)	31.30(4)
	3.96(7)	(1,0,1)	26.59(8)
	3.19(8)		
	3.04(9)		
		pGd	13.2^d
 H₃L₂^e	9.93(2)	(1,4,1)	37.74(4)
	9.75(4)	(1,2,1)	30.03(6)
	9.18(5)	(1,0,1)	21.22(5)
	4.26(5)		
	3.11(6)		
	2.77(7)		
		pGd	14.3
 NTP(PrHP)₃	9.95 ^f	(1,5,1)	42.8 ^g
	9.84 ^f	(1,4,1)	39.46 ^g
	9.09 ^f	(1,3,1)	35.69 ^g
	6.77 ^f	(1,2,1)	31.16 ^g
	3.81 ^f	(1,1,1)	26.35 ^g
	3.14 ^f	(1,0,1)	-
	2.76 ^f	(1,5,2)	65.3 ^g
		[1,3,2)	52.3 ^g
		pGd	12.3

^a $K_i = [\text{H}_i\text{L}]/[\text{H}_{i-1}\text{L}][\text{H}]$. ^b $\beta(\text{Gd}_m\text{H}_h\text{L}_l) = [\text{Gd}_m\text{H}_h\text{L}_l]/[\text{Gd}]^m[\text{H}]^h[\text{L}]^l$. ^c pGd value at pH = 7 ($\text{pGd} = -\log [\text{Gd(III)}]$), $\text{Cl} = 10^{-5}$ M, $\text{Cl}/\text{C}_{\text{Gd}} = 10$). ^d pGd at pH = 6. ^e in water, ref. 10. ^f in water, ref. 13. ^g in water, ref. 9.

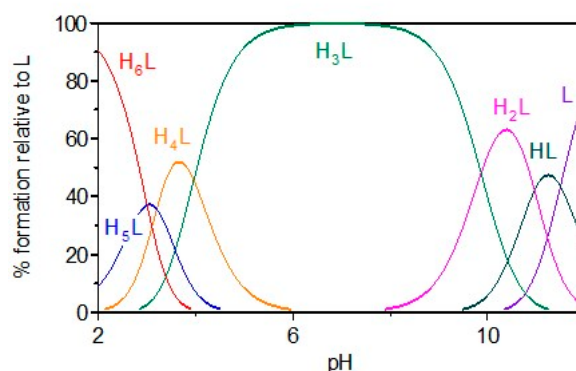


Figure 2. Species distribution curves of KEMPPr(3,4-HP)₃ ($C_L = 3.2 \times 10^{-4}$ M, 50% (w/w) DMSO/water medium).

Analysis of the potentiometric titration curves (Figure 1), namely that obtained for the Gd(III)/KEMPPr(3,4-HP)₃ system under 1:1 (Gd/L) stoichiometry, evidences a change in the deprotonation profile of the ligand due to its coordination to Gd(III). Since some precipitation was detected above pH = 6, the corresponding experimental points were not used in the calculations to obtain the Gd(III) complexation model. The obtained Gd(III) complexation model presents some similarities to that previously found for H₃L2 (see Table 1) [10], involving firstly the formation of a bis-chelated GdH₄L⁴⁺ species, a GdH₂L²⁺ tetra-chelated complex and afterwards the formation of a neutral hexa-coordinated GdL species. Analysis of the corresponding species distribution curves (Figure 3) shows that, under the used experimental conditions, the Gd(III) complexation begins below pH = 3, the bis-chelated complex is not very stable when compared with GdH₂L²⁺ or GdL, and the neutral GdL complex is the major complex species above pH ca 4.8.

The pGd value ($pGd = -\log [Gd(III)]$, $C_L = 10^{-5}$ M, $C_L/C_{Gd} = 10$) [17] contained in Table 1 for the Gd(III)/KEMPPr(3,4-HP)₃ system was calculated at pH 6, while those for the comparison compounds refer to pH = 7. Besides differences in the working media and pH, the pGd values obtained for KEMPPr(3,4-HP)₃ and H₃L2 show somewhat higher chelating capacity towards Gd(III) ($pGd = 13.2$ – 14.3) than for NTP(PrHP)₃ ($pGd = 12.3$). Therefore, it seems that the higher backbone rigidity and shorter arms of KEMPPr(3,4-HP)₃, when compared with H₃L2 or NTP(PrHP)₃, do not interfere on the Gd chelating ability of these tripodal 3,4-HP derivatives. In fact, there are other tripodal compounds that are stronger Gd chelators (pGd ca 19–20 at pH 7.4), which may be attributed to a better spatial arrangement in the coordination core around the metal ion, e.g. with 3,2-HOPO or pyrone moieties, as well as the standard Gd(III) ligands, diethylenetriamine penta-acetic acid (DTPA, $pGd = 19.1$) and 1,4,7,10-tetraazacyclododecane N,N',N'',N'''-tetra-acetic acid (DOTA, $pGd = 20.4$) at pH 7.4 [18–20].

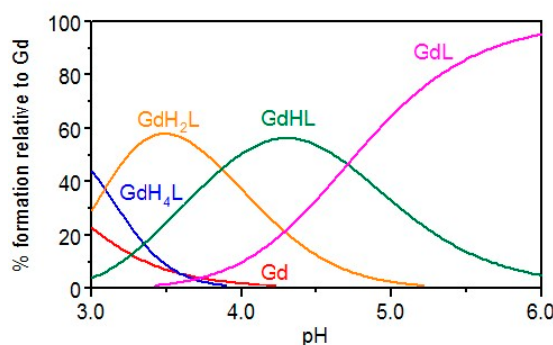


Figure 3. Species distribution curves for the Gd(III)/KEMPPr(3,4-HP)₃ 1:1 system ($C_L = 3.2 \times 10^{-4}$ M, 50% w/w DMSO/water medium).

2.2. Molecular Modeling of the Gd Complex

In order to get some insight on the molecular structure of the Gd complex and also to evaluate the possibility of enclosing water molecules in the Gd coordination shell, a prominent feature for its magnetic properties, DFT calculations were performed. Molecular simulations were obtained with full geometry optimization of the gadolinium complexes (with one or two water molecules coordinated to Gd) by quantum mechanical calculations based on DFT methods included in the Gaussian 03 software [21,22], with the B3LYP hybrid functional [23] and the Stuttgart/Dresden ECP (SDD) basis set [24]. No symmetry constraints were considered during geometry optimization in vacuum.

These calculations allowed to conclude that the Gd-KEMPPr(3,4-HP)₃ complex should present a distorted octahedral geometry with hexacoordination provided by the three bidentate 3,4-HOPO moieties of the ligand to Gd(III). The energy-minimized structure obtained for the 1:1 Gd complex with one coordinated water molecule is shown in Figure 4. Analysis of the model complex shows that the backbone cyclohexane ring (chair conformation) is in opposite direction relatively to the coordination core, seeming to be responsible by a certain degree of distortion of the Gd coordination geometry, which may also make difficult the coordination with another water molecule.

The coordination bond distances obtained for Gd-KEMPPr(3,4-HP)₃·1H₂O complex are 2.41(9) Å for Gd-O_{ligand} (average value and standard deviation) and 2.524 Å for Gd-O_{water}. These calculated distances for the Gd-O_{ligand} bonds agree well with previous results reported for GdL1.2H₂O (2.42(8) Å) [9], GdL2.1H₂O (2.39(9) Å) [10], GdL2.2H₂O (2.40(6) Å) [10] and the X-ray structure of the complex Gd(TREN-Me-3,2-HOPO)·2H₂O (average 2.38(3) Å) [18]. Relatively to the herein determined Gd-O_{water} bond length (2.524 Å), it can be concluded that it is also similar to already published ones: GdL1.2H₂O (average 2.58(7) Å) [9], GdL2.1H₂O (2.434 Å) [10] and GdL2.2H₂O (2.436 and 2.537 Å) [10], both ligands L1 and L2 presenting longer arms than KEMPPr(3,4-HP)₃ (7 against 5 atoms); even the values found in the X-ray structure of Gd(TREN-Me-3,2-HOPO)·2H₂O (2.436 and 2.446 Å) [18] (ligand with 4 atoms length arms) are under the same order of magnitude.

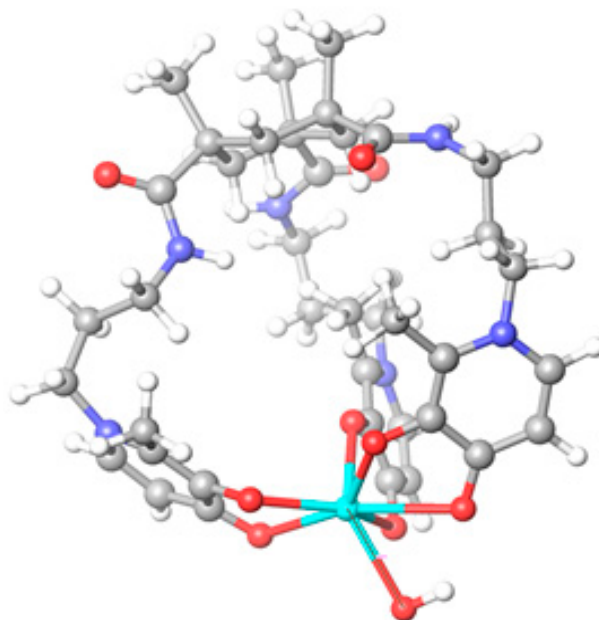


Figure 4. DFT-minimized structure of the Gd-KEMPPr(3,4-HP)₃·1H₂O complex, containing one water molecule in the coordination shell. Coloring of atoms: Gd (light blue), N (blue), O (red), C(grey) and H (white).

Even though two water molecules could be accepted to coordinate to the metal ion, these calculations suggested that a minimum energy complex structure only allowed the extra-

coordination of one water molecule to Gd, though the actual number of coordinated water molecules could only be experimentally obtained.

2.3. Predicted Pharmacokinetic Properties

The drug-likeness properties of the ligand KEMPPr(3,4-HP)₃ and its Si-KEMPPr(3,4-HP)₃ complex (as surrogate of the corresponding Gd complex) were predicted *in silico* using the software QikProp v.2.5 [25], after a prior optimization of their structures by energy minimization with Maestro program (see Section 2.3). The set of calculated pharmacokinetic properties and descriptors are summarized in Table 2. Analysis of these parameters, in comparison with commonly acceptable values for drugs, as described in the table footnotes [25], shows that the molecular weights (MW) are slightly higher than the commonly acceptable values for drugs (130-725), but the remaining pharmacokinetic parameters are within the range of the drug-like compounds, such as polar surface area (PSA), octanol/water partition coefficient (clog $P_{o/w}$), interaction with human serum albumin, brain–blood barrier (BBB) permeability, human oral absorption, while Caco-2 and MDCK cell permeability are also very good for the metal complex but poor for the ligand.

Table 2. Pharmacokinetic descriptors predicted in silico by QikProp v.2.5. [18].

Species	MW ^a	HB D/H BA ^b	PSA ^c	clog $P_{o/w}$ ^d	log K (HSA) Binding ^e	log BB ^f	Caco-2 Permeab (nm/s) ^g	MDCK Permeab (nm/s) ^h	% Oral Absorpt ⁱ
KEMPPr(HP) ₃	750.9	6/17	228.8	0.78	-0.97	-2.50	18	21	51
Si-KEMPPr(HP) ₃	778.9	3/14	133.5	3.51	-0.34	-0.80	1212	1490	93

^a Molecular weight (acceptable range: from 130 to 725). ^b number of hydrogen bond donors (HBD, acceptable from 0 to 6) and hydrogen bond acceptors (HBA, acceptable from 2 to 20). ^cPSA (van der Waals surface area of polar nitrogen and oxygen atoms) (acceptable range: from 7 to 200). ^d Predicted octanol/water partition coefficient clog $P_{o/w}$ (acceptable range: from -2.0 to 6.5). ^e Interaction with human albumin (acceptable range: from -1.5 to +1.5). ^f Brain–blood barrier permeability (acceptable range: from -3.0 to +1.2). ^g Predicted Caco-2 cell permeability in nm/s (acceptable range: 25 is poor and >500 is great). ^h Predicted MDCK cell permeability in nm/s (acceptable range: <25 is poor and >500 is great). ⁱ Percentage of human oral absorption (acceptable range: <25% is poor and >80% is high).

2.4. Biodistribution Studies

In the absence of lab facilities to evaluate the *in vivo* MRI properties and biodistribution of the Gd-KEMPPr(3,4-HP)₃ complex [26], the biodistribution and excretion profiles of the analogue ⁶⁷Ga-KEMPPr(3,4-HP)₃ complex, as a surrogate of the Gd complex, were evaluated in CD-1 mice at 30 min, 1 h and 24 h after administration of the radiotracer (Figures 5 and 6), similarly to previously reported by us [11]. We have decided to carry out this study considering the importance of the biodistribution and clearance profiles of Gd contrast agents to assess their potential as imaging probes, especially due to the known risk of nephrogenic systemic fibrosis (NSF) associated to GBCAs. Similar approaches have been recently reported [27] in which a complex of DTPA with ⁸⁶Y, a radionuclide used for positron emission tomography (PET) was used to evaluate the biodistribution and clearance in rats, as a surrogate of the corresponding Gd complex to bring prospect for multimodality molecular imaging.

Data from these studies demonstrate a fast blood clearance and a rapid washout from the main organs and tissues since the % I.A./organ is lower than 1% for all major organs, except for the kidney, at 24 h post- injection (p.i.). The highest uptake in the kidneys and the high excretion rate of

radioactivity from the whole animal body (65.4 ± 1.1 , 81.1 ± 0.1 and 91.2 ± 0.9 % I.A. at 30 min, 1 h and 24 h, respectively) indicate that the complex is predominantly eliminated by the urinary pathway.

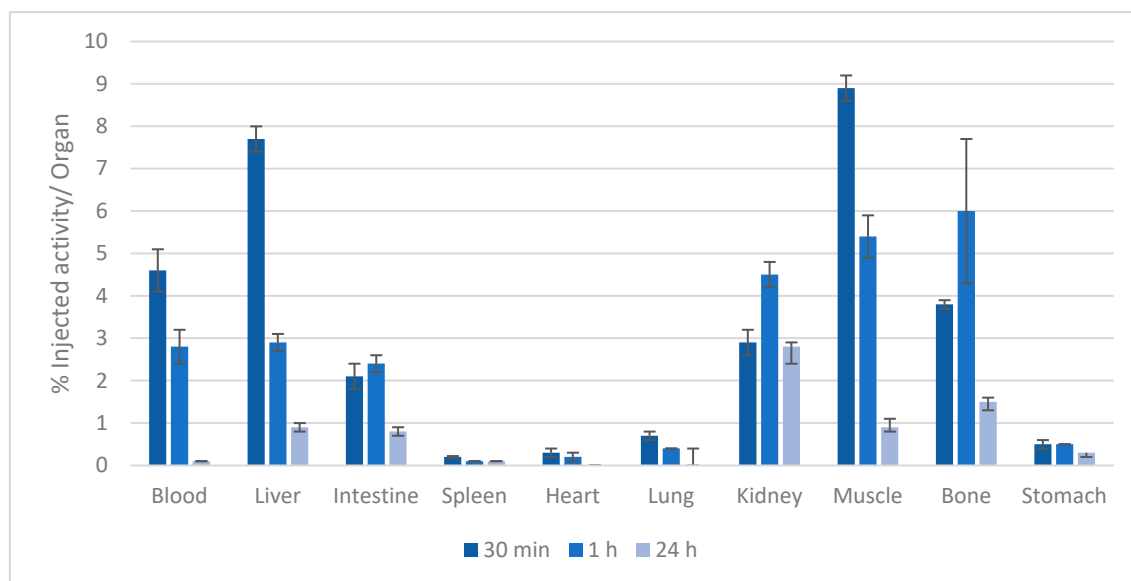


Figure 5. Biodistribution of ^{67}Ga -KEMPPr(3,4-HP)₃ in CD1 mice, at 30 min, 1 h and 24 h after administration.

The results of these studies suggest a high *in vivo* stability of the ^{67}Ga -KEMPPr(3,4-HP)₃ complex, as the biodistribution pattern related to the main radiochemical impurity species (^{67}Ga hydroxides ($\text{Ga}(\text{OH})_3$ and $\text{Ga}(\text{OH})_4^-$ and free $^{67}\text{Ga}^{3+}$) is well established and was not found.

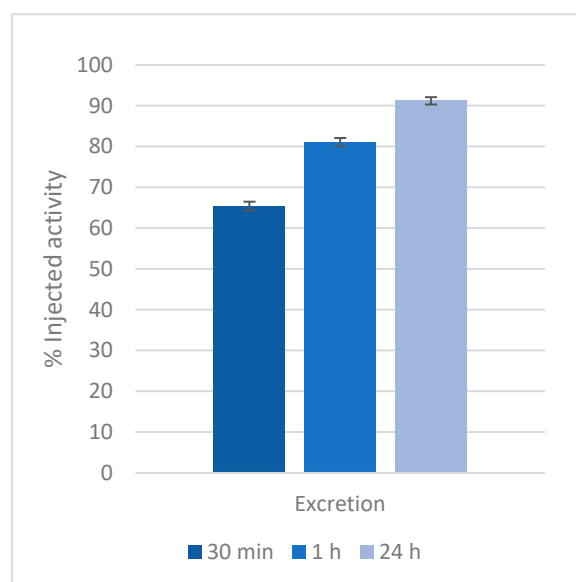


Figure 6. Total excretion of ^{67}Ga -KEMPPr(3,4-HP)₃ from whole animal body, at 30 min, 1 h and 24 h after administration in CD1 mice.

Overall, these *in vivo* studies show a favorable biodistribution profile of this ^{67}Ga -KEMPPr(3,4-HP)₃ complex, with no relevant uptake in any organ except the excretion path at 24 h p.i., high *in vivo* stability and rapid excretion from the animal body.

3. Materials and Methods

3.1. Gd Complexation Studies

3.1.1. Materials and Equipment

The compound KEMPPr(3,4-HP)₃ was synthesized according to previously published procedure [11]. The GdCl₃ stock solution (9.8×10^{-3} M) was prepared from the gadolinium salt in HCl 0.1 M medium, to avoid hydrolysis, and standardized by inductively coupled plasma emission (ICP). The 0.1 M HCl solution used in the calibration of the glass electrode was obtained from a Titrisol ampoule. The precise amount of HCl of the Gd(III) solution was determined by the standard-addition method using 0.1 M HCl (Titrisol). The titrant solution used in the potentiometric titrations was obtained from a carbonate-free 0.1 M KOH commercial ampoule (Titrisol) and standardized by titration with potassium hydrogen phthalate, being rejected whenever the percentage of carbonate (Gran's method) [28] was higher than 1% of the total amount of base. The potentiometric studies were performed with an automated potentiometric apparatus containing a Crison micropH 2002 milivoltmeter, a Crison microBu 2031 burette and a Haake thermostatic bath ($T = 25.0 \pm 0.1$ °C), controlled by PASAT program. The glass and Ag/AgCl reference electrodes were previously conditioned in different DMSO/water mixtures of increasing DMSO % composition (till 50%) and the answer of the glass electrode was measured through determination of the Nernst parameters by Gran's method [28] obtained from strong acid–strong base (HCl/KOH) calibrations.

3.1.2. Potentiometric Measurements

Potentiometric titrations of compound KEMPPr(3,4-HP)₃, in the absence or presence of Gd(III), were performed in 50% (w/w) DMSO/water medium at ionic strength (*I*) 0.1 M KCl, $T = 25.0 \pm 0.1$ °C, using 0.1 M KOH titrant. Each titration was repeated three times, for which the total volume was 20 mL, the total concentration of ligand (*C_L*) 3.2×10^{-4} M and the Gd³⁺/KEMPPr(3,4-HP)₃ molar ratios 0:1 and 1:1.

3.1.3. Calculation of Equilibrium Constants

The stepwise protonation constants, $K_i = [\text{H}_i\text{L}]/[\text{H}_{i-1}\text{L}][\text{H}]$, and the global Gd(III) complex stability constants, $\beta(\text{Gd}_m\text{H}_n\text{L}) = [\text{Gd}_m\text{H}_n\text{L}]/[\text{Gd}]^m[\text{H}]^n[\text{L}]$, were calculated by fitting the potentiometric data with the Hyperquad software [12]. The gadolinium hydrolysis model was determined under the same experimental conditions (50% (w/w) DMSO/water medium, $I = 0.1$ M KCl, $T = 25.0 \pm 0.1$ °C) and the values obtained for the stability constants ($\log \beta(\text{GdH}_2) = -15.17$, $\log \beta(\text{GdH}_3) = -24.06$) were included in the equilibrium model as well as the value of ionic product of water K_w ($10^{-14.95}$). The species distribution curves were obtained with the Hyss program [12].

3.2. Molecular Modeling

Molecular modeling studies were performed to get an insight on the molecular structure of the Gd(III) complex of KEMPPr(3,4-HP)₃ and also to anticipate the most probable number of water molecules coordinated to gadolinium. The studies were achieved with full geometry optimization of the gadolinium complexes by quantum mechanical calculations based on density functional theory (DFT) methods included in the Gaussian 03 software [21,22], with the B3LYP hybrid functional [23] and the Stuttgart/Dresden (SDD) effective core potential (ECP) basis set [24]. No symmetry constraints were used during geometry optimization.

3.3. In Silico Evaluation of Pharmacokinetic Parameters

The pharmacokinetic parameters for the ligand KEMPPr(3,4-HP)₃ and its Si-complex (as a surrogate of the Gd-complex due to the software non-recognition of Gd) were calculated using the

QikProp v.2.5. program [25], contained in the Maestro software [29]. The chemical structures of the ligand and complex were energy-minimized before being submitted to these calculations.

3.4. Biodistribution Studies

Animal studies were carried out in conformity with the national law and with the European Union (EU) Guidelines for Animal Care and Ethics in Animal Experimentation by properly accredited researchers by the national authorities. The animals were housed in a temperature and humidity-controlled room with a 12 h light/dark schedule in animal house facilities approved by Portuguese Authority of Food and Veterinary (DGAV) and maintained on a normal diet *ad libitum*.

The biodistribution of ^{67}Ga -KEMPPr(3,4-HP)₃ was evaluated in groups of three female CD-1 mice (randomly bred, Charles River) weighing approximately 25–28 g each. The animals were injected intravenously with 100 μL (5–10 MBq) of ^{67}Ga -citrate via the tail vein and immediately after with 0.5 μmol of the ligand in 100 μL of saline solution. The mice were sacrificed by cervical dislocation at different time points (30 min, 1 h and 24 h) post-injection. The injected radioactive dose and the radioactivity remaining in the animal after sacrifice were measured using a dose calibrator (Capintec). The difference between the radioactivity in the injected and sacrificed animal was assumed to be due to total excretion from the whole animal body. Blood samples were taken by cardiac puncture at sacrifice. Then, tissue samples of the main organs were dissected, weighed and measured using a gamma counter (Berthold). The biodistribution results were expressed as the percentage of the injected activity per organ (% I.A.).

4. Conclusions

Our goal was to investigate some relevant physico-chemical and biological properties of a new Gd(III) complex in view of the potential interest of this chelate as a MRI contrast probe. The hexadentate tripodal ligand (H₃L, KEMPPr(3,4-HP)₃), containing three 3,4-HOPO bidentate chelating moieties attached to a tri-carboxylic-cyclohexane-based backbone (KEMP acid), demonstrated a good capacity for wrapping and hexa-coordinating Gd(III), thus leaving free sites for extra coordination with water molecules. In particular, the results of solution equilibrium studies confirmed the formation of GdL complexes with high thermodynamic stability ($\log \beta(\text{GdL}) = 26.59$; $\text{pGd} = 13.2$). Molecular simulation of the Gd complex indicated a slightly distorted octahedral coordination with one water molecule in the inner metal coordination, a relevant feature for the magnetic properties of this chelate. These results, together with the favorable *in vivo* stability and biodistribution profile of the complex, indicate potential prospective interest of this Gd-chelate for future developments towards new MRI agents. Although further investigation is required, as *in vitro* ^{17}O nuclear magnetic resonance (^{17}O NMR) and nuclear magnetic relaxation dispersion (NMRD) studies to evaluate the actual number of water molecules in the inner coordination sphere and the proton relaxivity, we hope that the herein presented results may serve as a useful tool for medicinal chemists to design and create additional MRI contrast agents.

Author Contributions: Conceptualization: M.A.S. and S.C.; methodology, S.C. and L.G.; software, I.D. and S.C.; investigation, I.D. and L.G.; resources, L.G., S.C. and M.A.S.; data curation, I.D., L.G. and S.C.; writing—original draft preparation, S.C. and M.A.S.; writing—review and editing, I.D., L.G., S.C. and M.A.S.; supervision, S.C. and M.A.S. All authors have read and agreed to the published version of the manuscript.

Funding: Centro de Química Estrutural is a Research Unit funded by FCT through projects UIDB/00100/2020 (<https://doi.org/10.54499/UIDB/00100/2020>) and UIDP/00100/2020 (<https://doi.org/10.54499/UIDP/00100/2020>). Institute of Molecular Sciences is an Associate Laboratory funded by FCT through project LA/P/0056/2020 (<https://doi.org/10.54499/LA/P/0056/2020>).

Ethical statement: Animal study was conducted in accordance with the principles of laboratory animal science on animal care, protection and welfare and complies with national legislation and institutional requirements. The experimental procedures were approved by the Portuguese Authority (DGVA) as well as

the animal facilities and the researchers responsible for the animal experimentation (Ref: 520/000/000/2004 and DGV_9112009).

Institutional Review Board Statement: Not applicable.

Informed Consent Statement: Not applicable.

Data Availability Statement: Data are contained only within the article.

Conflicts of Interest: The authors declare no conflicts of interest.

References

1. Wahsner, J.; Gale, E.M.; Rodríguez-Rodríguez, A.; Caravan, P. Chemistry of MRI contrast agents: current challenges and new frontiers. *Chem. Rev.* **2019**, *119*, 957–1057. <https://doi.org/10.1021/acs.chemrev.8b00363>
2. Aime, S.; Crich, S.G.; Gianolio, E.; Giovenzana, G.B.; Tei, L.; Terreno, E. High sensitivity lanthanide(III) based probes for MR-medical imaging. *Coord. Chem. Rev.* **2006**, *250*, 1562–1579. <https://doi.org/10.1016/j.ccr.2006.03.015>
3. Villaraza, A.J.L.; Bumb, A.; Brechbiel, M.W. Macromolecules, Dendrimers, and Nanomaterials in Magnetic Resonance Imaging: The Interplay between Size, Function, and Pharmacokinetics. *Chem. Rev.* **2010**, *110*, 2921–2959. <https://doi.org/10.1021/cr900232t>
4. Cheng, S.; Abramova, L.; Gaab, G.; Turabelidze, G.; Patel, P.; Arduino, M.; Hess, T.; Kallen, A.; Jhung, M. Nephrogenic Fibrosing Dermopathy Associated With Exposure to Gadolinium-Containing Contrast Agents - St. Louis, Missouri, 2002-2006. *J. Am. Med. Assoc.* **2007**, *297*, 1542–1544. <https://doi.org/10.1001/jama.297.14.1542>
5. Uzal-Varela, R.; Rodríguez-Rodríguez, A.; Wang, H.; Esteban-Gómez, D.; Brandariz, I.; Gale, E.M.; Caravan, P.; Platas-Iglesias, C. Prediction of Gd(III) complex stability. *Coord. Chem. Rev.* **2022**, *467*, 214606. <https://doi.org/10.1016/j.ccr.2022.214606>
6. Prybylski, J.P.; Semelka, R.C.; Jay, M. The stability of gadolinium-based contrast agents in human serum: a re-analysis of literature data and association with clinical outcomes. *Magn. Reson. Imag.* **2017**, *38*, 145–151. <https://doi.org/10.1016/j.mri.2017.01.006>
7. Werner, E.J.; Avedano, S.; Botta, M.; Hay, B.P.; Moore, E.G.; Aime, S.; Raymond, K.N. Highly soluble tris-hydroxypyridonate Gd(III) complexes with increased hydration number, fast water exchange, slow electronic relaxation, and high relaxivity. *J. Am. Chem. Soc.* **2007**, *129*, 1870–1871. <https://doi.org/10.1021/ja068026z>
8. Pierre, V.C.; Melchior, M.; Doble, D.M.J.; Raymond, K.N. Toward optimized highrelaxivity MRI agents: thermodynamic selectivity of hydroxypyridonate /catecholate ligands. *Inorg. Chem.* **2004**, *43*, 8520–8525. <https://doi.org/10.1021/ic0493447>
9. Mendonça, A.C.; Martins, A.F.; Melchior, A.; Marques, S.M.; Chaves, S.; Villette, S.; Petoud, S.; Zanonato, P.L.; Tolazzi, M.; Bonnet, C.S.; Tóth, É.; Di Bernardo, P.; Geraldès, C.F.G.C.; Santos, M.A. New tris-3,4-HOPO lanthanide complexes as potential imaging probes. Complex stability and magnetic properties. *Dalton Trans* **2013**, *42*, 6046–6057. <https://doi.org/10.1039/C2DT32237D>
10. Chaves, S.; Gwizdała, K.; Chand, K.; Gano, L.; Pallier, A.; Tóth, É.; Santos, M.A. Gd^{III} and Ga^{III} complexes with a new tris-3,4-HOPO ligand, towards new potential imaging probes: complex stability, magnetic properties and biodistribution. *Dalton Trans.* **2022**, *51*, 6436–6447. <https://doi.org/10.1039/D2DT00066K>
11. Grazina, R.; Gano, L.; Sebestik, J.; Santos, M.A. New tripodal hydroxypyridinone based chelating agents for Fe(III), Al(III) and Ga(III): Synthesis, physico-chemical properties and bioevaluation. *J. Inorg. Biochem.* **2009**, *103*, 262–273. <https://doi.org/10.1016/j.jinorgbio.2008.10.014>

12. Gans, P.; Sabatini, A.; Vacca, A. Investigation of equilibria in solution. Determination of equilibrium constants with the HYPERQUAD suite of programs. *Talanta* **1996**, *43*, 1739–1753. [https://doi.org/10.1016/0039-9140\(96\)01958-3](https://doi.org/10.1016/0039-9140(96)01958-3)
13. Chaves, S.; Marques, S.M.; Matos, A.M.F.; Nunes, A.; Gano, L.; Tuccinardi, T.; Martinelli, A.; Santos, M.A. New Tris(hydroxypyridinones) as Iron and Aluminium Sequestering Agents: Synthesis, Complexation and In Vivo Studies. *Chem. Eur. J.* **2010**, *16*, 10535–10545. <https://doi.org/10.1002/chem.201001335>
14. Pawlak, Z.; Bates, R.G. Solute-solvent interactions in acid-base dissociation: nine protonated nitrogen bases in water-DMSO solvents. *J. Sol. Chem.* **1975**, *4*, 817–829. <https://doi.org/10.1007/BF00650538>
15. Malla, B.; Neeraja, R.; Kumar, J.S.; Ramanaiah, M. An eletrometric method for the determination of impact of DMSO-water mixtures on pKa values of salicylic acid derivatives. *Int. J. App. Pharm.* **2023**, *15*, 309–314. <https://doi.org/10.22159/ijap.2023v15i6.49253>
16. Beck, M.T.; Nagypal, I. Chemistry of complex equilibria, Ellis Horwood Ltd, Chichester, **1990**, ISBN 13-173063-0.
17. Raymond, K.N., Carrano, C.J. Coordination chemistry and microbial iron transport. *Acc. Chem. Res.* **1979**, *12*, 183–190. <https://doi.org/10.1021/ar50137a004>
18. Xu, J.; Franklin, S.J.; Whisenhunt Jr., D.W.; Raymond, K.N. Gadolinium complex of tris[(3-hydroxy-1-methyl-2-oxo-1,2-didehydropyridine-4-carboxamido)ethyl]- amine: A New Class of gadolinium magnetic resonance relaxation agents. *J. Am. Chem. Soc.* **1995**, *117*, 7245–7246. <https://doi.org/10.1021/ja00132a025>
19. Puerta, D.T.; Botta, M.; Jocker, C.J.; Werner, E.J.; Avedano, S.; Raymond, K.N.; Cohen, S.M. Tris(pyrrone) Chelates of Gd(III) as High Solubility MRI-CA. *J. Am. Chem. Soc.* **2006**, *128*, 2222–2223. <https://doi.org/10.1021/ja057954f>
20. Werner, E.J.; Datta, A.; Jocher, C.J.; Raymond, K.N. High-Relaxivity MRI Contrast Agents: Where Coordination Chemistry Meets Medical Imaging. *Angew. Chem. Int. Ed.* **2008**, *47*, 8568–8580. <https://doi.org/10.1002/anie.200800212>
21. Parr, R.G.; Yang, W. *Density Functional Theory of Atoms and Molecules*, Oxford University Press, New York, **1989**.
22. Frisch, M.J.; Trucks, G.W.; Schlegel, H.B.; Scuseria, G.E.; Robb, M.A.; Cheeseman, J.R.; Montgomery Jr., J.A.; Vreven, T.; Kudin, K.N.; Burant, J.C.; Millam, J.M.; Iyengar, S.S.; Tomasi, J.; Barone, V.; Mennucci, B.; Cossi, M.; Scalmani, G.; Rega, N.; Petersson, G.A.; Nakatsuji, H.; Hada, M.; Ehara, M.; Toyota, K.; Fukuda, R.; Hasegawa, J.; Ishida, M.; Nakajima, T.; Honda, Y.; Kitao, O.; Nakai, H.; Klene, M.; Li, X.; Knox, J.E.; Hratchian, H.P.; Cross, J.B.; Bakken, V.; Adamo, C.; Jaramillo, J.; Gomperts, R.; Stratmann, R.E.; Yazyev, O.; Austin, A.J.; Cammi, R.; Pomelli, C.; Ochterski, J.W.; Ayala, P.Y.; Morokuma, K.; Voth, G.A.; Salvador, P.; Dannenberg, J.J.; Zakrzewski, V.G.; Dapprich, S.; Daniels, A.D.; Strain, M.C.; Farkas, O.; Malick, D.K.; Rabuck, A.D.; Raghavachari, K.; Foresman, J.B.; Ortiz, J.V.; Cui, Q.; Baboul, A.G.; Clifford, S.; Cioslowski, J.; Stefanov, B.B.; Liu, G.; Liashenko, A.; Piskorz, P.; Komaromi, I.; Martin, R.L.; Fox, D.J.; Keith, T.; Al-Laham, M.A.; Peng, C.Y.; Nanayakkara, A.; Challacombe, M.; Gill, P.M.W.; Johnson, B.; Chen, W.; Wong, M.W.; Gonzalez, C.; Pople, J.A. Gaussian 03, Revision C.02, Gaussian, Inc., Wallingford CT, **2004**.
23. Bauschlicher, C.W. A comparison of the accuracy of different functionals. *Chem. Phys. Lett.* **1995**, *246*, 40–44. [https://doi.org/10.1016/0009-2614\(95\)01089-R](https://doi.org/10.1016/0009-2614(95)01089-R)

24. (a) Haussermann, U.; Dolg, M.; Stoll, H.; Preuss, H.; Schwerdtfeger, P.; Pitzer, R.M. Accuracy of energy-adjusted quasirelativistic ab initio pseudopotentials. *Mol. Phys.* **1993**, *78*, 1211–1224. <https://doi.org/10.1080/00268979300100801> (b) Kuchle, W.; Dolg, M.; Stoll, H.; Preuss, H. Energy-adjusted pseudopotentials for the actinides. Parameter sets and test calculations for thorium and thorium monoxide. *J. Chem. Phys.* **1994**, *100*, 7535–7542. <https://doi.org/10.1063/1.466847> (c) Leininger, T.; Nicklass, A.; Stoll, H.; Dolg, M.; Schwerdtfeger, P. The accuracy of the pseudopotential approximation. II. A comparison of various core sizes for indium pseudopotentials in calculations for spectroscopic constants of InH, InF, and InCl. *J. Chem. Phys.* **1996**, *105*, 1052–1059. <https://doi.org/10.1063/1.471950>
25. QikProp, version 2.5, Schrödinger, LLC, New York, NY, **2005**.
26. Thompson, M.K.; Misselwitz, B.; Tso, L.; Doble, D.M.J.; Schmitt-Willich, H.; Raymond, K.N. In Vivo Evaluation of Gadolinium Hydroxypyridonate Chelates: Initial Experience as Contrast Media in Magnetic Resonance Imaging. *J. Med. Chem.* **2005**, *48*, 3874–3877. <https://doi.org/10.1021/jm049041m>
27. Le Fur, M.; Rotile, N.J.; Correcher, C.; Jordan, V.C.; Ross, A.W.; Catana, C.; Caravan, P. Yttrium-86 is a Positron Emitting Surrogate of Gadolinium for Noninvasive Quantification of Whole-Body Distribution of Gadolinium-Based Contrast Agents. *Angew. Chem. Int. Ed.* **2020**, *59*, 1474–1478. <https://doi.org/10.1002/anie.201911858>
28. Rossotti, F.J.C.; Rossotti, H. Potentiometric titrations using Gran plots: a textbook omission. *J. Chem. Ed.* **1965**, *42*, 375–378. <https://doi.org/10.1021/ed042p375>
29. Maestro, version 9.3. Schrödinger Inc., Portland, OR, **2012**.

Disclaimer/Publisher's Note: The statements, opinions and data contained in all publications are solely those of the individual author(s) and contributor(s) and not of MDPI and/or the editor(s). MDPI and/or the editor(s) disclaim responsibility for any injury to people or property resulting from any ideas, methods, instructions or products referred to in the content.